

three most intense lines whose resolution is more or less obvious agree within experimental error with the predictions from the potassium term values: we conclude that our interpretation is correct and that the wave-length positions of all the lines are known. The components are readily sketched in the figure with the obvious additional criterion that the sum of the component ordinates at a given wave-length must equal the observed intensity. It is gratifying that all of the observed intensity is accounted for satisfactorily by component lines whose relative intensities decrease gradually to zero. The relative intensities of these lines are 100 : 34 : 18 : 8.5, etc.

It is of interest to note that the corrected width of an absorption line gives directly the width of the initial state if the final state width is negligible. Many solid absorbers have prominent and easily measurable absorption lines (sometimes called "white lines" in photographic

studies) and, when applicable, this direct method of determining the width of a  $K$  or an  $L$  state may be very convenient.

In the absorption curve of a solid absorber we expect to find on the short wave-length side of the main edge resonance absorption lines more or less perturbed by overlapping wave functions from neighboring atoms. We also expect to find resonance absorption bands due to transitions to the allowed Brillouin energy bands.<sup>11</sup> The resolution of these resonance lines and bands into the component structure, which would yield very significant information about the solid, demands first a determination of the contour of the main edge. It is evident from the analysis of the argon curve and from the additional complications of the solid structure that the meaning of the main edge for a solid absorber is rather obscure.

<sup>11</sup> A typical absorption curve for a solid absorber, the  $L_{III}$  region for silver, is reproduced in Fig. 5 of reference 5.

## Nuclear Energy Levels in $B^{10}$ <sup>1</sup>

P. GERALD KRUGER, F. W. STALLMANN AND W. E. SHOUPP<sup>2</sup>  
*Department of Physics, University of Illinois, Urbana, Illinois.*

(Received June 16, 1939)

Five thousand stereoscopic pictures of electron tracks in a cloud chamber yielded six hundred sixty-five Compton electrons from a thin mica foil and seventy-six  $\pm$  electron pairs formed in the gas in the chamber. These data indicate thirty-one lines in the  $\gamma$ -ray spectrum of  $B^{10}$ . Nine energy levels account for the observed lines in a satisfactory manner, and are not in disagreement with the neutron spectrum from the same reaction. An attempt to correlate the observed energy levels with those predicted by theory leads to the following suggested classification:  $^3S_1$  as the ground state (relative energy zero);  $^3D_{123}$  at 0.26, 0.50 and 0.61 Mev;  $^1S$  at 1.44 Mev;  $^1D$  at 1.93 Mev;  $^3D$  at 2.92 Mev;  $^1D$  at 3.64 Mev; and  $^3F$  at 4.73 Mev.

**A** PREVIOUS<sup>3</sup> examination of the  $\gamma$ -rays from  $B^{10}$  showed the presence of six  $\gamma$ -ray lines which could be correlated with the neutron data of Bonner and Brubaker.<sup>4</sup> However, the prob-

<sup>1</sup> A preliminary report of part of these data was given at the Washington meeting of the American Physical Society, Phys. Rev. **55**, 1129(A) (1939).

<sup>2</sup> Fellow at the Westinghouse Research Laboratory since September 1938.

<sup>3</sup> P. G. Kruger and G. K. Green, Phys. Rev. **52**, 773 (1937).

<sup>4</sup> T. W. Bonner and W. M. Brubaker, Phys. Rev. **50**, 308 (1936).

able error in the lines reported was of the order of 0.1 Mev and the resolution of the method poor, so that it was impossible to say if more than six  $\gamma$ -ray lines were present. For that reason the experiment has been repeated under conditions which give better resolution and higher accuracy of the measurement of  $\gamma$ -ray energies.

There are two convenient ways of measuring  $\gamma$ -ray energies: the Compton recoil electron method and the  $\pm$  electron pair production

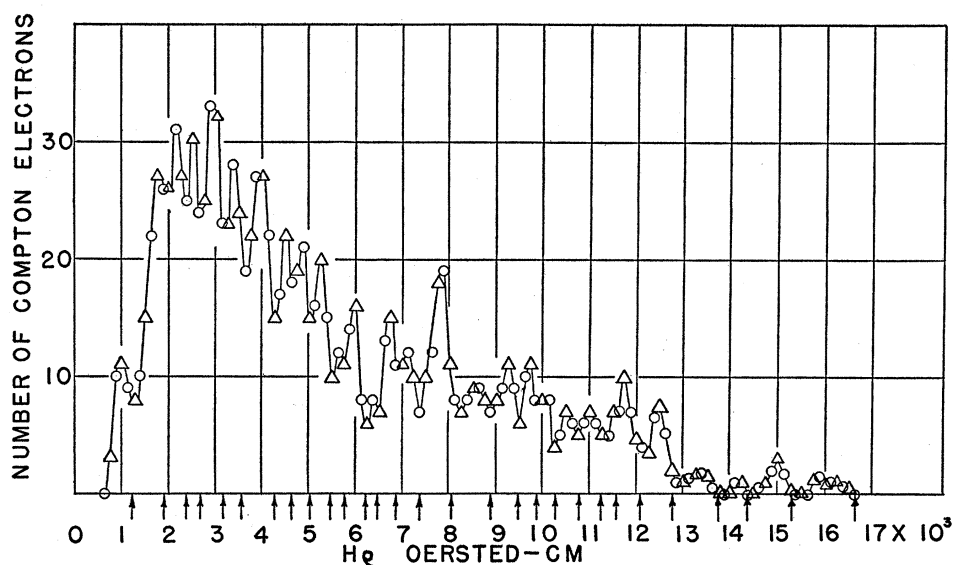


FIG. 1. Momentum distribution for Compton electrons ejected from a 50-mg/cm<sup>2</sup> mica foil by  $\gamma$ -rays from B<sup>10</sup>.

method. Both have disadvantages. The Compton recoil method has the inherent disadvantage of straggling effects in the conversion foil, but must be used for  $\gamma$ -ray energies below  $2 mc^2$ , and is best below 1.5 Mev unless the  $\gamma$ -ray lines are very intense. If a thin foil of material of large atomic number is used for  $\pm$  electron pair production, there exists the same disadvantage of straggling. However,  $\pm$  pair electrons produced in a gas do not suffer straggling and thus, a study of their energies will yield the most accurate results for  $\gamma$ -ray energies above  $2 mc^2$ . With these ideas in mind both methods have been used to study the  $\gamma$ -rays of B<sup>10</sup>. Below 1.16 Mev the Compton electron method has been used, whereas above 1.16 Mev the  $\pm$  electron pair data are considered best, though the Compton data in that region agree with the  $\pm$  electron pair data as well as can be expected.

Increased accuracy has been attained by taking stereoscopic pictures of the electron tracks and by carefully collimating the  $\gamma$ -ray beam. Stereoscopic pictures enable a more rigid selection of tracks, so that, in the case of Compton recoil electrons one can be sure that the electrons emerge in the forward direction within  $\pm 10^\circ$  to the direction of the incident  $\gamma$ -rays and that both Compton electrons and  $\pm$  pair electrons lie in the plane of the cloud chamber i.e., that the plane

of the track is perpendicular to the magnetic field.

The collimation of the  $\gamma$ -ray beam was affected by placing a lead block six inches thick between the beryllium target and the cloud chamber and aligning a suitable hole in the lead block in such a way that the hole allowed free passage only to  $\gamma$ -rays which filled the solid angle subtended by the cloud chamber at the target. This prevents, to a large extent, the entrance of scattered  $\gamma$ -rays into the cloud chamber and together with the more rigid selection of tracks made possible by stereoscopic pictures, has greatly increased the resolving power of the method.

A rough consideration of the effects of small angle scattering on the path of an electron through a gas led to the conclusion that air was approximately the best gas to use in the chamber for the  $\pm$  electron pair production method. Though the probability of  $\pm$  electron pair production increases with  $Z^2$  so does the small angle scattering. Thus the choice of a suitable gas must be made on the basis of selecting the gas which will give a satisfactory yield and not too much error due to scattering. Air meets these conditions well, the predicted probable error in the  $\gamma$ -ray energy from one  $\pm$  electron pair measurement being about  $\pm 5$  percent. Thus only a few pairs per  $\gamma$ -ray line must be observed in order to have  $\gamma$ -ray energies accurate to plus-

minus a few hundredths of a million electron volts.

The beryllium target, which was bombarded with 0.96 Mev deuterons, was placed in the end of the beam exit tube of the cyclotron. The cloud chamber was positioned so that its center was on a line perpendicular to the direction of incident deuterons. This allowed room to place a 2½'' thick lead shield between the cloud chamber and the cyclotron chamber to reduce the background radiation from the cyclotron. The cloud chamber was 20 cm in diameter, 2.5 cm deep and was filled with air and alcohol vapor at atmospheric pressure. The Helmholtz coils gave a magnetic field of about 1500 oersteds which was constant over the sensitive volume of the cloud chamber to ±0.5 percent. The Helmholtz coil current was read for every expansion and the magnetic field calculated for each track measured.

The Compton electrons were ejected from a 50-mg/cm<sup>2</sup> mica foil placed in the cloud chamber perpendicular to the line connecting the Be target and the chamber center.

For measuring the tracks, their stereoscopic images were projected, by the optical system used during photography, on a fine ground glass screen which could be clamped in place once the track images were in coincidence. The radii of curvature were measured by a special measuring engine built for the purpose. The engine was built so that three points could be brought in coincidence with the circular track and the length of the chord defined by the two end-points as well as the sagitta read off directly. From these data the radius is readily calculated. The accuracy of measurement of the engine was checked by measuring circles of known radii of curvature. The result showed that the readings are reliable to less than ±0.5 percent.

The momentum distribution of the six hundred sixty-five Compton recoil electrons is shown in Fig. 1. There each circle represents the number of electrons observed in  $H\rho$  intervals of 250 oersted-cm. The triangles represent the number of electrons in  $H\rho$  intervals of the same size but overlapping the first set by  $H\rho=125$  oersted-cm.

TABLE I. *Gamma-ray lines in the B<sup>10</sup> spectrum.*

$H\rho$ OERSTED CM	$E_C$ MEV	$E_p$ MEV	RELATIVE INTENSITY	$E_{CALC}$ MEV	TRANSITION		
1,250	0.25		60	0.24 & 0.26	$B_2 - B_1$	$B_1 - A$	
1,900	0.41		120	0.49 & 0.35		$D - C$	$B_3 - B_1$
2,400	0.55		160	0.50		$B_2 - A$	
2,700	0.63		130	0.61		$B_3 - A$	
3,200	0.77		160	0.72		$F - E$	
3,600	0.89		140	0.94		$C - B_2$	
4,300	1.08		170	1.09 & 0.99		$G - F$	$E - D$
4,650	1.19	1.16	120	1.18		$C - B_1$	
5,050	1.31	1.33	120	1.32		$D - B_3$	
5,500	1.44	1.43	100	1.48, 1.43 & 1.44	$E - C$	$D - B_2$	$C - A$
5,800	1.52	1.57	35				
6,250	1.66	1.68	70	1.67		$D - B_1$	
6,500	1.74	1.80	70	1.81 & 1.71		$G - E$	$F - D$
6,900	1.85						
7,400	1.99	1.91	25	1.93		$D - A$	
8,100	2.20		2.11	20			
		2.24	8	2.20		$F - C$	
		2.31	20	2.31		$E - B_3$	
8,900	2.44	2.45	40	2.42		$E - B_2$	
9,500	2.63	2.64	40	2.66		$E - B_1$	
9,900	2.74	2.78	30	2.80		$G - D$	
10,300	2.89	2.91	30	2.92		$E - A$	
10,800	3.01	3.00	22	3.03		$F - B_3$	
11,300	3.15		20	3.14		$F - B_2$	
11,600	3.25	3.25	4	3.29		$G - C$	
12,100	3.40	3.38	50	3.38		$F - B_1$	
12,800	3.62	3.66	40	3.64		$F - A$	
13,800	3.92	3.90	10				
14,400	4.12	4.15	4	4.12		$G - B_3$	
		4.24	1	4.23		$G - B_2$	
15,300	4.35	4.46	12	4.47		$G - B_1$	
16,600	4.74	4.71	7	4.73		$G - A$	

TABLE II. Gamma-ray energies as deduced from the measurements on  $\pm$  electron pairs formed in an air-filled cloud chamber.

Below are listed the $h\nu$ values in Mev corresponding to each pair observed.													
	1.120	1.307	1.427	1.545	1.639	1.792	1.911	2.134	2.242	2.320	2.424	2.613	2.770
	1.157	1.339	1.420	1.584	1.679	1.826	1.903	2.078		2.316	2.480	2.671	2.786
	1.190	1.308	1.446	1.596	1.685	1.848				2.283		2.626	
	1.145	1.273	1.467	1.538	1.674	1.749				2.300			
	1.124	1.350	1.402		1.704					2.343			
	1.191	1.378	1.417										
	1.164	1.339	1.413										
	1.176	1.355											
		1.313											
		1.320											
No of pr. per line	8	10	7	4	5	4	2	2	1	5	2	3	2
Average value of $h\nu$	1.158	1.328	1.427	1.566	1.676	1.804	1.907	2.106	2.242	2.312	2.452	2.637	2.778
Diff. between extreme $h\nu$ values per line	0.071	0.105	0.065	0.058	0.065	0.099	0.008	0.056		0.060	0.056	0.058	0.016
	2.910	3.004	3.263	3.355	3.622	3.864	4.127	4.238	4.395	4.648	5.478	6.064	6.481
	2.918		3.241	3.412	3.700	3.930	4.175		4.513	4.704			
							4.139		4.481	4.770			
No. of pr. per line	2	1	2	2	2	2	3	1	3	3			
Average value of $h\nu$	2.914	3.004	3.252	3.383	3.661	3.897	4.147	4.238	4.463	4.707			
Diff. between extreme $h\nu$ values per line	0.008		0.022	0.057	0.078	0.066	0.048		0.118	0.122			

The minima<sup>3</sup> between peaks give the  $H\rho$  values for the  $\gamma$ -ray lines and are indicated in Fig. 1 with arrows. The corresponding values are listed in Table I, column one, and are used to calculate the  $\gamma$ -ray energies with the formula:

$$h\nu_{\gamma} = mc^2 \left[ \frac{1 + (1 + A^2)^{\frac{1}{2}}}{2A} - \frac{1}{2} \right],$$

where

$$A = mc^2 / eH\rho.$$

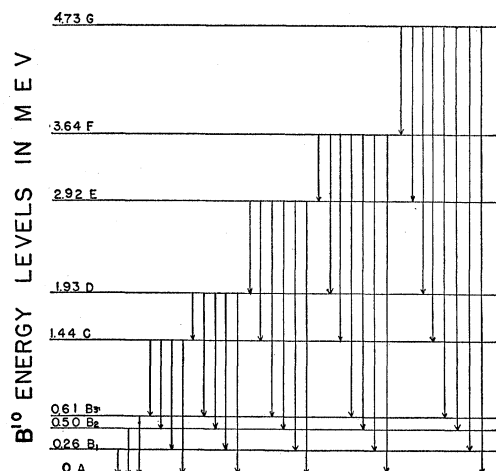


FIG. 2. Nuclear energy levels in  $B^{10}$ . Gamma-ray energies used in developing this term system have been obtained from measurements on  $\pm$  pair electrons for gamma-ray energies larger than 1.16 Mev. Below 1.16 Mev the measurements from Compton electron have been used.

The energies of the  $\gamma$ -rays, thus calculated, are given in column two ( $E_c$ ) of Table I.

The energy of a  $\gamma$ -ray which produces a  $\pm$  electron pair is given by  $h\nu_{\gamma} = 2mc^2 + KE^- + KE^+$ , where

$$KE^{\pm} = mc^2 [(B^2 + 1)^{\frac{1}{2}} - 1]$$

and

$$B = H\rho e / mc^2.$$

The  $\gamma$ -ray energies corresponding to the seventy-six observed pairs which represent twenty-three  $\gamma$ -rays of energy above 1.16 Mev are given in Table II. As the tabulation shows, the energy spread for any one  $\gamma$ -ray line is approximately 0.06 Mev. In most cases this is less than the expected spread of  $\pm 5$  percent due to small angle scattering. The discrepancy may be explained partly by the careful selection of tracks. The average values of the  $\gamma$ -ray lines in Table II are listed for comparison in column three ( $E_p$ ) of Table I.

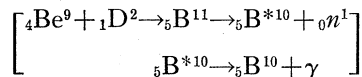
From the observed thirty-one  $\gamma$ -ray lines the energy level system shown in Fig. 2 has been deduced. For comparison with the observed  $\gamma$ -ray energies, the differences between the energy levels are tabulated in column five of Table I. Four lines have been used twice and one line three times but this represents no difficulty since the lines calculated from the term system are so nearly alike that they could not be resolved by the present method. This is particularly true in

the low energy region where the energy values depend on Compton electrons. Line 1.80 Mev may be double with values 1.77 Mev and 1.84 Mev as can be seen by examining the pair energies for this line in Table II. Arbitrary term designations *A*, *B*<sub>1</sub>, *B*<sub>2</sub>, *B*<sub>3</sub>, *C*, *D*, *E*, *F*, *G*, have been given the energy levels in Fig. 2. The corresponding transitions for the lines are given in column six of Table I.

All but three lines (1.57, 2.11, and 3.90 Mev) of Table I have been used. Here it is to be noted that lines 1.57 Mev and 2.11 Mev have a sum equal to 3.68 Mev which is near the term value 3.64 Mev. This may indicate another level at 1.57 Mev or 2.11 Mev. There is no indication of a possible place for the line 3.90 Mev.

The intensities of the lines given in column four of Table I are the average of the intensities as deduced from the Compton electrons and the ± pair electron. To get the intensities from the Compton electrons the curve in Fig. 1 was reduced according to the process previously described.<sup>3</sup> The relative intensity of the lines as deduced from ± electron pairs was obtained by taking into account the probability of pair production at various energies.

If the term system in Fig. 2 is correct there should be evidence for more neutron groups from this reaction



than were reported by Bonner and Brubaker.<sup>4</sup>

TABLE III. Intensity correlation between the neutron spectrum and the γ-ray spectrum.

TERM	A Σ γ-RAY OUT OF LEVEL	B Σ γ-RAY INTO LEVEL	C NEUTRON POPULA- TION	$\frac{B+C}{A}$
<i>F</i>	335	85	320	$\frac{405}{335} = 1.2$
<i>E</i>	225	195	55	$\frac{250}{225} = 1.1$
<i>D</i>	405	150	170	$\frac{320}{405} = 0.8$
<i>C</i>	280	140	120	$\frac{260}{280} = 0.9$
<i>B</i>	350	770	640	$\frac{1410}{350} = 4.0$

Such evidence is found in the excellent results of Staub and Stephens.<sup>5</sup> Their curves\* (Figs. 1 and 2) are shown in Fig. 3 after being redrawn slightly.

By assuming *Q*=4.18 Mev and the values of the energy levels as deduced from our γ-rays (Fig. 2), the energy of the neutron groups which should be observed for Staub and Stephens' energy of incident deuterons, can be calculated. The position of these neutron groups is shown by the arrows along the energy axis in Fig. 3. It is seen that all of the predicted groups which can be resolved are present, though the position of the groups does not agree well with the predicted

<sup>5</sup> H. Staub and W. E. Stephens, Phys. Rev. **55**, 131 (1939).

\* The authors wish to express their thanks to Dr. W. E. Stephens for making the original data for these curves available to them.

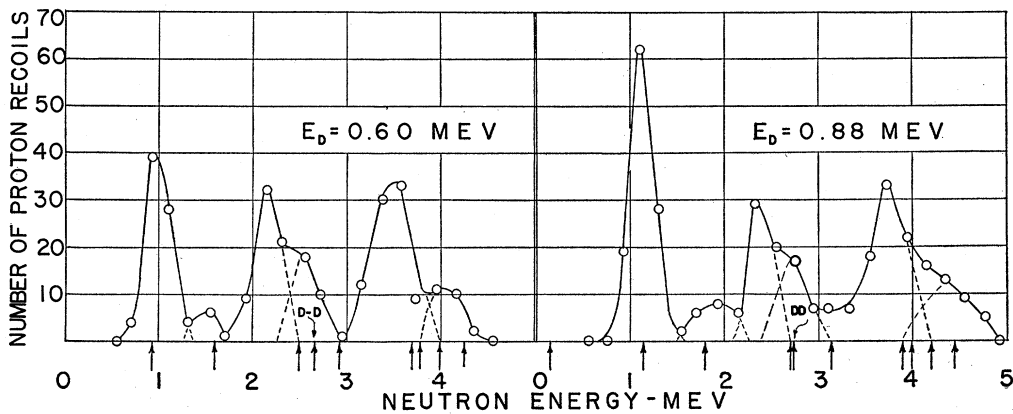


FIG. 3. Neutron spectrum from the reaction  ${}_4\text{Be}^9 + {}_1\text{D}^2 \rightarrow {}_5\text{B}^{10} + {}_0n^1$  for two energies of incident deuterons (0.60 and 0.88 Mev). Data from Staub and Stephens.

position. This may be due to errors in the range energy curve, stopping power values, or inadequate corrections.

Staub and Stephens expressed the view that the neutron group at approximately 3.00 Mev was due to D-D contamination neutrons. This can hardly be true in view of the fact that the intensity ratio of the two neutron peaks at approximately 2.50 Mev and 3.00 Mev for the two energies of incident deuterons (0.6 and 0.88 Mev) remains nearly constant whereas the excitation functions for the two reactions vary greatly for the two energies. Moreover, the position of the D-D neutron group, indicated by the arrows marked D-D in Fig. 3, and calculated for their energy of incident deuteron does not fit the 3.00 Mev peak. Thus, it seems clear that the D-D contamination neutrons cannot be present in their experiment in large numbers, and that the 3.00 Mev peak really corresponds to neutrons leaving the B<sup>10</sup> nucleus in the 1.44 Mev level.

Now it is possible to obtain the areas under the neutron peaks and thus get an idea of the initial neutron population of the levels and to compare that with the observed  $\gamma$ -ray intensities. The intensity check which should be observed is

$$\frac{(\sum \gamma\text{-ray intensities} + \sum \text{neutron population})_{\text{in}}}{(\sum \gamma\text{-ray intensities})_{\text{out}}} = 1.$$

The results are shown in Table III. The agree-

ment is good except for the B level and the discrepancy there is due to the low intensity of lines 0.63, 0.55 and 0.25 Mev. It is possible that these lines obtained much too low an intensity due to successive subtraction of straggling tails from the peaks at higher energy during the reduction process of the curve in Fig. 1.

Feenberg and Wigner,<sup>6</sup> and Feenberg and Phillips<sup>7</sup> have made theoretical calculations concerning the type and position of terms in the B<sup>10</sup> nucleus. An attempted correlation between the theoretical levels and the observed levels leads to the following: A, B<sub>1</sub>, B<sub>2</sub>, B<sub>3</sub>, C, D, E, F, G are, respectively, <sup>3</sup>S<sub>1</sub>; <sup>3</sup>D<sub>1</sub>, <sup>3</sup>D<sub>2</sub>, <sup>3</sup>D<sub>3</sub>, <sup>1</sup>S<sub>0</sub>; <sup>1</sup>D<sub>2</sub>; <sup>3</sup>D; <sup>1</sup>D and <sup>3</sup>F. This gives a ratio

$$\frac{\text{calculated sing.-trip. splitting}}{\text{observed sing.-trip. splitting}} \cong 2.3,$$

which is fairly constant for the suggested classification.

It is impossible to make a further check on the classification at this time by using the intensities of the various lines. Many more pairs and Compton electrons will need to be observed before the intensities are sufficiently accurate for such a check.

The authors wish to express their thanks to Professor R. Serber for many helpful discussions.

<sup>6</sup> E. Feenberg and E. Wigner, Phys. Rev. **51**, 95 (1937).

<sup>7</sup> E. Feenberg and M. Phillips, Phys. Rev. **51**, 597 (1937).